IEEE/CSC & ESAS European Superconductivity News Forum (ESNF), No. 14, October 2010
The published version of this manuscript appeared in *IEEE Transactions on Applied Superconductivity* **21**, Issue 3, 3301 - 3306 (2011)

AC Loss Reduction in Filamentized YBCO Coated Conductors with Virtual Transverse Cross-cuts

Yifei Zhang *Member IEEE*, Robert C. Duckworth, Tam T. Ha, Frederick A. List III, Michael J. Gouge, Yimin Chen, Xuming Xiong, Venkat Selvamanickam, and Anatolii Polyanskii

***Abstract*—While the performance of $YBa_2Cu_3O_{7-x}$ (YBCO)-based coated conductors under dc currents has improved significantly in recent years, filamentization is being investigated as a technique to reduce ac loss so that the 2nd generation (2G) high temperature superconducting (HTS) wires can also be utilized in various ac power applications such as cables, transformers and fault current limiters. Experimental studies have shown that simply filamentizing the superconducting layer is not effective enough to reduce ac loss because of incomplete flux penetration in between the filaments as the length of the tape increases. To introduce flux penetration in between the filaments more uniformly and reduce the ac loss, virtual transverse cross-cuts were made in superconducting filaments of the coated conductors fabricated using the metal organic chemical vapor deposition (MOCVD) method. The virtual transverse cross-cuts were formed by making cross-cuts (17 ~ 120 μm wide) on the IBAD (ion beam assisted deposition)-MgO templates using laser scribing followed by depositing the superconducting layer (~ 0.6 μm thick). AC losses were measured and compared for filamentized conductors with and without the cross-cuts under applied peak ac fields up to 100 mT. The results were analyzed to evaluate the efficacy of filament decoupling and the feasibility of using this method to achieve ac loss reduction.**

***Index Terms*—AC Loss, Coated Conductor, Filamentization, YBCO.**

I. INTRODUCTION

IN the last several years, great progress has been made in the R&D of the coated conductor technology by which long-length high temperature superconducting (HTS) wires are fabricated. The second generation (2G) HTS wire technology utilizes different approaches such as RABiTS™ (Rolling Assisted Biaxially Textured Substrates) or IBAD (Ion Beam Assisted Deposition) for the preparation of a template on which high performance HTS films, mostly YBCO-based, are deposited. While the self-field dc critical current (I_c, 77 K) of the best coated conductors has exceeded 1,000 A/cm-w for short samples, long-length (up to 1 kilometer) wires with the YBCO-based layer deposited by MOCVD (Metal Organic Chemical Vapor Deposition) are commercially available, having a self-field I_c of 250 ~ 300 A/cm-w [1]. The improved conductor performance is enabling the use of 2G wires in many electrical power devices.

However, for most of the applications such as cables, transformers and fault current limiters, ac loss remains a concern. AC loss is generated within the 2G wires by ac transport currents and/or ac magnetic fields. With respect to the ac applied fields, the high ac loss of a coated conductor is related to its high aspect ratio geometry with the hysteresis ac loss in perpendicular fields becoming a significant portion of the total ac loss. Dividing a coated conductor tape into narrower filaments has been proven to be a promising approach to reduce the ac loss [2-4]. Various techniques have been investigated for filamentizing coated conductors [5-7]. In order to reduce the ac loss effectively, it is required that the HTS filaments be fully decoupled not only electrically but also magnetically. The magnetic decoupling requires magnetic flux penetration in between the filaments. While magnetic flux can penetrate through the ends of a short filamentary sample, field penetration is problematic for long tapes as the flux can be blocked by the HTS filaments. One method to accomplish the field penetration in these HTS filaments is through the twisting of the tapes as proposed by Oberly [8] or through the transposition of the slanted filaments in two electrically connected tapes as done by Tsukamoto and Abraimov [9-10]. With the flat tape geometry, it was proposed earlier by Ashworth [11] that the field penetration for long tapes could be achieved by introducing periodic transverse cross-cuts in the HTS layer of a coated conductor. The non-superconducting cross-cut works as a channel for the penetration of flux and the stabilizing normal metal above the cross-cut serves as a bridge maintaining a continuous current path. The practicality of this approach depends on the tradeoff between the hysteresis ac loss reduction due to the enhanced decoupling and the introduced resistive loss at the metallic bridges, and the ability to translate this approach to long-length, high throughput production of 2G wires.

In this study, we proposed and investigated a different method to make the transverse cross-cuts in the production process of YBCO coated conductors. Instead of direct cutting

Manuscript received 3 August 2010. This work was sponsored by the U.S. DOE Office of Electricity Delivery and Energy Reliability - Advanced Cables and Conductors Program under contract DE-AC05-00OR22725 with Oak Ridge National Laboratory, managed and operated by UT-Battelle, LLC.

Y. Zhang, R. C. Duckworth, T. T. Ha, F. A. List and M. J. Gouge are with Oak Ridge National Laboratory, Oak Ridge, TN 37831 (phone: +1-865-241-8337; fax: +1-865-576-7770; e-mail: zhangyf@ornl.gov).
Y. Chen and X. Xiong are with SuperPower Inc., Schenectady, NY 12304.
V. Selvamanickam is with SuperPower Inc. as well as University of Houston, Houston, TX 77004 (email: selva@superpower-inc.com).

on the HTS layer after the YBCO coated conductor is produced, a cross-cut was made on the buffered template by laser scribing, as shown in Fig. 1. Following the laser scribing of the buffer was the deposition of the HTS layer and the silver layer, step (2) and (3) in Fig. 1. Due to the defective buffer surface at the scribing, the microstructure of the HTS film right above the cut was disrupted. In this way, a virtual cross-cut was formed in the HTS layer. The longitudinal direction filamentization, step (4), was also done by laser scribing. Using samples of different geometries and configurations, the effect of the virtual cross-cut on magnetic field penetration and ac loss was investigated. To simulate long-length tapes, short samples with non-filamentized parts at the ends were used and compared with the fully filamentized samples. AC losses were measured for these samples to evaluate the effectiveness of the cross-cut approach.

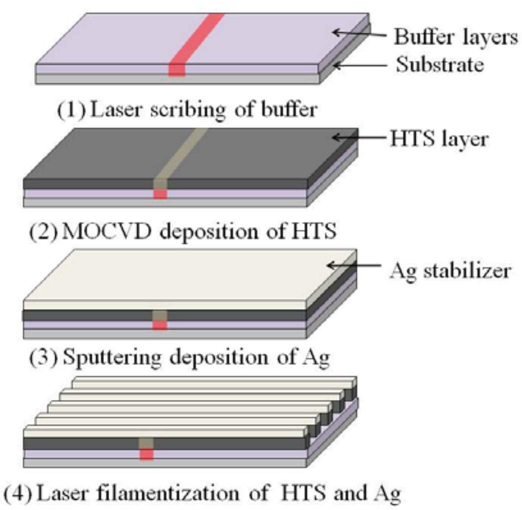

Fig. 1. Procedure for making a filamentized coated conductor sample with a virtual transverse cross-cut. In this case, the sample is fully filamentized or the filamentization is from end to end.

II. Experimental Details and Techniques

A. Production of Virtual Cross-Cut

The IBAD-MgO template used for this study was prepared by SuperPower Inc., Schenectady, NY. In brief, the standard 12 mm wide template has a structure of $LaMnO_3$ (LMO) / Homo-epi-MgO / IBAD-MgO / Y_2O_3 / Al_2O_3 / Hastelloy. The thickness of the LMO layer is 30 nm.

Transverse cross-cuts on the surface of the template were made by laser scribing using a QuikLaze-50 Nd:YAG laser machining system manufactured by New Wave Research. The system is a TriLite model and equipped with an automatic sample stage. For the scribing of the IBAD-MgO template, the 352 nm green light was selected. At a fixed pulse rate of 20 Hz, the depth of the scribing can be adjusted by changing the laser power output as well as the sample stage motion speed. The width of the scribing was varied from 17 µm to 120 µm by tuning the aperture in the beam line.

Deposition of high performance Zr-doped GdYBCO films was done by SuperPower using the MOCVD approach. The HTS layer deposition was followed by the sputtering deposition of a silver layer (1.5 µm thick) which serves as the stabilizer. After the silver deposition, all coated conductor tapes were oxygen annealed before further processing or measurements. In cases when the GdYBCO layer was deposited on a template having a transverse cross-cut, a virtual cross-cut was formed in the HTS film due to the disruption of the underneath LMO buffer by the laser scribing.

The same laser system used for making the cross-cuts on the buffered template was also used for the filamentization of the coated conductor tapes. The filamentization was along the longitudinal direction of a tape. Processing parameters of the laser system were set such that the scribing is through the GdYBCO layer. The width of the laser scribing for the filamentization was around 100 µm. As 10 filaments were formed in the 1.2 cm wide tape, each filament was about 1.1 mm wide. After the laser filamentization, all samples were oxygen annealed at 500 °C for 2 hours in a tube furnace. The purpose of this procedure is to remove the electrical coupling of the filaments from the laser processing as shown by Levin [4].

Fig. 2 shows the geometries of different samples used for the magnetic field penetration study and for the ac loss measurements. The five different samples are: (A) an as-received control sample; (B) an end-to-end fully filamentized sample; (C) a close-end filamentized sample without cross-cut; (D) a close-end filamentized sample with a cross-cut in the center; and (E) A close-end filamentized sample with a cross-cut near the end of the filaments. For the sample D or E that had a cross-cut, the width of the cross-cut was 30 µm. Depending on the filamentization configuration and whether there was a virtual cross-cut, the field penetration and ac loss were expected to be different.

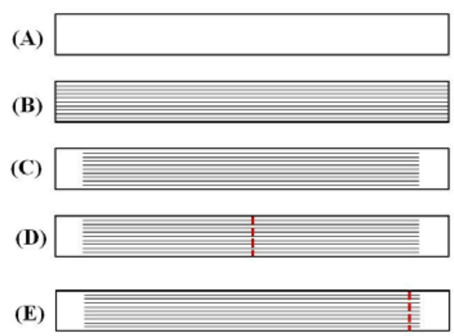

Fig. 2. Schematic geometries of the samples (10×1.2 cm) used for the magnetic field penetration and ac loss studies. The non-filamentized regions at the ends of samples (C), (D) and (E) were all 1 cm long. The locations of the virtual cross-cuts in sample D and E were indicated by the dashed lines.

B. Characterization of Virtual Cross-Cut Conductors

Critical currents (I_c) were measured using the standard four-probe method for the as-received tapes and the filamentized samples without the cross-cuts. The measurements were carried out at 77 K with samples immersed in liquid nitrogen. The criterion for determining I_c values was 1 µV/cm. For the as-received 0.6 µm thick GdYBCO tapes, the measured self-field dc critical current (I_c, 77 K) was around 280 A. After the filamentization, the measured I_c was around 235 A. Using the same system, the voltage-current (V-I) relationships of the samples having cross-cuts were also measured. With the two voltage taps sitting across the scribing, the resistance was determined from the slope of the V-I curve.

Using two different methods, the effect of a virtual transverse cross-cut on magnetic field penetration was investigated by measuring the field distribution when an ac perpendicular field was applied. For a 10×1.2 cm sample, the first method to understand the nature of field penetration utilized five small pick-up coils that were positioned on the tape surface and in the middle of the sample. The coils were distributed along the length and the two coils at the ends were both 1 cm away from the end of the tape. The spacing between two adjacent pick-up coils was 2 cm. Under a peak ac field of 15 mT at 50 Hz, the induced voltage in each of the pick-up coils was measured using a lock-in amplifier.

The effect of a virtual cross-cut on magnetic field penetration in between the filaments was also characterized using magneto-optical imaging (MOI). While an MOI sample is only 1.2×1.2 cm in size, the sample geometries were similar to that used for the field profile measurements with the pick-up coils. The non-filamentized regions at the ends of the two samples similar to (C) and (D) in Fig. 2 were 2 mm long in this case.

With respect to ac loss characterization, dc magnetization versus magnetic field (*M-H*) loops were measured for samples with different geometries using a commercial SQUID-based magnetometer, a Quantum Design model MPMS-7, to further understand the effect of the cross-cut on the decoupling of the filaments. With a perpendicular maximum field up to 100 mT, the integral of an *M-H* loop was analyzed for the evaluation of the ac loss and the comparison of the different geometries. The size of a magnetic measurement sample was 5×4 mm. The non-filamentized regions at the ends of the two samples similar to (C) and (D) in Fig. 2 were 1 mm long in this case to reflect to the end effects

AC losses of the samples were measured as functions of peak ac field as well as field frequency using a calorimetric method [7]. The measurements were carried out at 77 K with a sample immersed in liquid nitrogen. A thermometer was located in the center of the sample measured. To calibrate the generated heat, a resistive heater that was made from twisted copper wire was bonded to the sample with epoxy and the sample assembly was placed in between two Styrofoam blocks. Using a solenoid magnet, a perpendicular ac field up to 100 mT and up to 120 Hz can be applied. The calibrated relationship between the thermometer response and the power input of the heater was used to calculate the heat generation when an ac field was applied. The energizing of the calibration heater and the applying of the ac field were both 5 seconds long. The heat pulse was repeated several times to generate good statistics on the thermometer response to different heat loads with a long enough time interval between any two pulses for the sample temperature to return to equilibrium. The ac loss sample size was also 10×1.2 cm and the geometries were same as those shown in Fig. 2.

Finally, the microstructure of the GdYBCO film was studied with a focus on how the laser scribing on the LMO buffer layer changes the HTS film structure. Cross-sectional TEM microscopy was used to compare the structure of the high quality GdYBCO in the normal region with the disrupted structure right above the cross-cut.

III. Results and Discussion

A. *Resistance of a Virtual Transverse Cross-Cut*

All V-I curves obtained from the samples having virtual cross-cuts showed ohmic behaviors. Fig. 3 shows how the resistance changes with the width of the cross-cut on the LMO buffer. The width of a cross-cut was measured using optical microscopy as well as a surface profilometer. Here, the width of the laser scribing was varied from 30 µm to 120 µm. Also shown in the plot as the solid line is the resistance calculated assuming that there is a 1.5 µm thick silver bridge right above the virtual cross-cut. The electrical current flows through the silver bridge at the virtual cross-cut. Based on the thickness of the silver and an estimated contact resistance of 1×10^{-8} Ω-m^2 between the Ag and the HTS film, the calculated transfer length is about 7.5 µm. Then, the length of the bridge is determined by adding two transfer lengths (one at each end of the bridge) to the measured length of the cross-cut. The measured resistance is higher than the calculated values, suggesting that the effective length of the bridge could be longer than the measured width of the transverse cross-cut on the buffer due to the interface characteristics. The important element to emphasize is that there is a linear dependence of the resistance of the virtual cross cut on the width of the virtual transverse cross-cut.

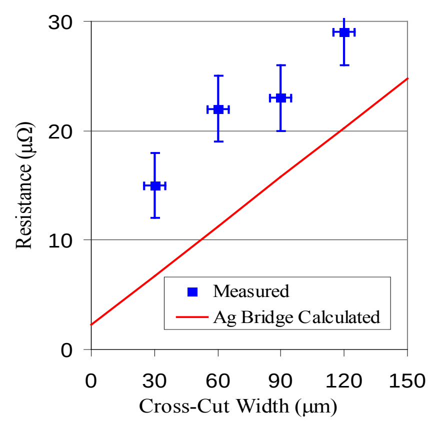

Fig. 3. Resistance across the virtual cross-cut as a function of the width of the cross-cut. The measurement was carried at 77 K in liquid nitrogen and the voltage tap spacing was 4 mm.

The resistance of a virtual cross-cut is an important parameter as it determines the resistive loss, the tradeoff in implementing the cross-cut approach for reducing total ac loss. For practical consideration, this resistance should be minimized by minimizing the width of the cross-cut.

B. *Microstructure of a Virtual Cross-Cut*

The formation of a virtual cross-cut in the HTS film is simply due to the defective buffer surface produced by the laser scribing. Using this method, the disruption of the HTS film structure is much easier than scribing directly into the superconducting layer where the thickness of the film is another parameter. The microstructure of the GdYBCO film was inspected using the cross-sectional transmission electron microscopy (TEM). In Fig. 4(a), the Z-contrast image obtained from within the virtual cross-cut clearly showed that the microstructure of the GdYBCO film is random and defective. As a comparison, the GdYBCO film in a normal region which is away from the cross-cut has very good epitaxial structure, as shown in Fig. 4(b).

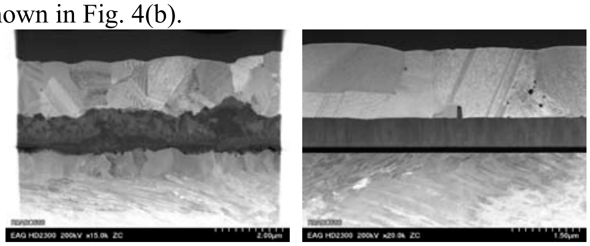

Fig. 4. Cross-sectional TEM Z-contrast images obtained from (a) a region within the virtual cross-cut, and (b) a region that is away from the cross-cut, showing the difference in the microstructures of the GdYBCO film.

C. Magnetic Field Penetration

Magnetic field profiles were measured using five pick-up coils that were positioned on the sample surface and distributed along the length. Fig. 5 shows the field profiles of the four samples with different geometries as shown in Fig. 2. It is evident that the virtual cross-cut facilitated the magnetic flux penetration so that sample D had similar field profile as sample B which was fully filamentized from end to end. On the contrary, sample C which was not fully filamentized and had no cross-cut showed a similar field profile as that for the control sample A.

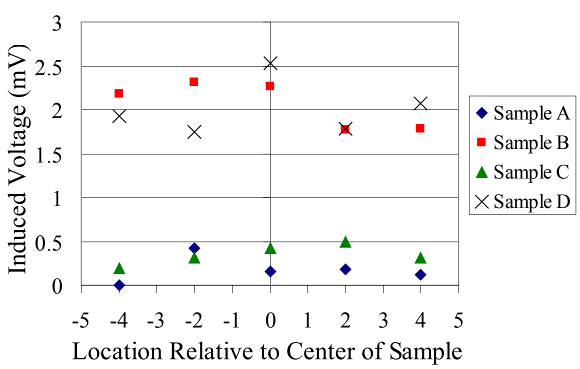

Fig. 5. Magnetic field profiles represented by the induced voltage from the pick-up coils obtained as a perpendicular peak ac field of 15 mT at 50 Hz was applied to the samples of different geometries. The horizontal axis indicates the relative locations of the pick-up coils.

The effect of the cross-cut on field penetration was also evident from the results of the MOI inspection. Fig. 6 shows the MOI images of the two samples with and without a cross-cut. The images were taken when the samples were zero-field cooled (ZFC) to 10 K and under an applied field of 80 mT. As both the samples were not fully filamentized, magnetic fluxes were blocked from entering in between the filaments through the ends. For the sample that had a cross-cut across the width, the field penetration was greatly enhanced.

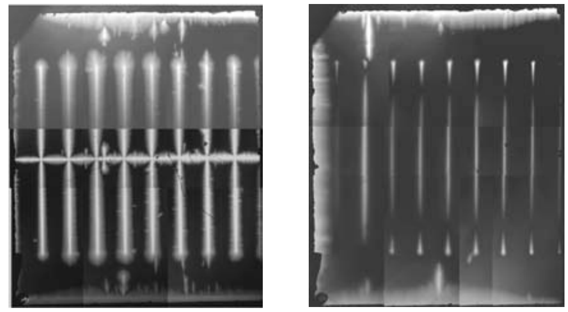

(a) (b)

Fig. 6. MOI images showing the difference in magnetic flux penetration between sample (a) which had a virtual cross-cut, and sample (b) which had no cross-cut. The sample geometries were similar to that of sample C and D shown in Fig. 2. The top and bottom non-filamentized regions were both 2 mm long.

D. DC Magnetization (M-H Loop)

Samples used for dc magnetization measurements had similar geometries as those shown in Fig. 2 but smaller size. The measurements were carried out at 77 K with perpendicular applied fields up to 100 mT. The *M-H* loops of the four different samples are shown in Fig. 7. The integral of an *M-H* loop, which is the loss per volume per cycle, is given by

$$W = \mu_0 \oint M(H_a)dH_a \qquad (1)$$

where M is the magnetization and H_a is the applied magnetic field. The calculated losses are 5.66, 1.14, 4.05, and 1.07 J/cm^3/cycle for A, B, C, and D, respectively. This result is consistent with the field penetration observation.

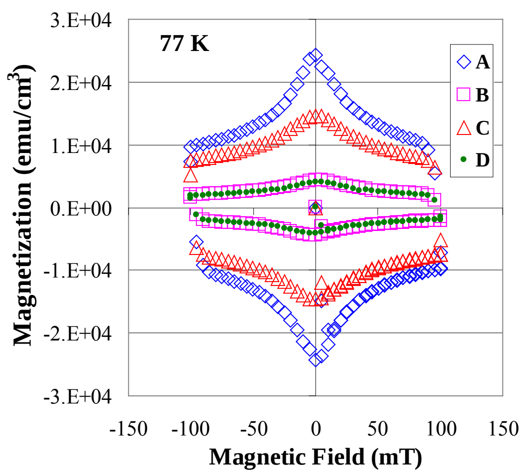

Fig. 7. *M-H* loops obtained from the dc magnetization measurements using a SQUID magnetometer at 77 K with perpendicular applied fields up to 100 mT for the four samples of different geometries.

E. AC Losses

Fig. 8 shows the ac loss measurement results for samples A, B, C, and D. The geometries of the four samples are indicated in Fig. 2. For the non-filamentized control sample A, the ac loss was high up to about 10 W/m at a peak perpendicular field of 100 mT. The ac losses of the fully filamentized sample B were about a factor of five lower than that of sample A. The close-end filamentized sample C without a cross-cut had relatively higher ac losses at lower peak fields, but with the increasing of the peak field, the ac loss increase of this sample decreased. This was likely due to the flux penetration through the ends of the sample as the magnetic field increased. In comparison to the other three samples, sample D, which was not fully filamentized but had a cross-cut, showed the highest ac loss. This high ac loss appeared to be inconsistent with the result of the field penetration study, suggesting that it might be caused by different heating mechanism.

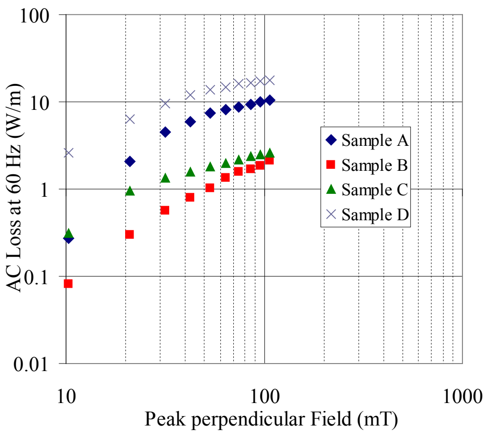

Fig. 8. AC loss measurement results of the four samples A, B, C, and D that had different geometries. The configurations of the samples are indicated in Fig.2.

To understand the "abnormal" high ac loss of sample D which had a virtual cross-cut at its center, further experimental measurements were carried out on samples with modified configurations. First, using chemical etching with 1:1 NH_4OH and H_2O_2 solution, the silver bridge right above the cross-cut of sample D was removed. The new sample after the silver removal was denoted as sample D*. The ac loss of sample D* was measured and is shown in Fig. 9. It can be seen that the ac loss dropped significantly after the silver removal. This change in the ac loss suggested that the measured total ac loss of sample D was mainly the resistive loss that was generated in the silver bridge due to the induced circulating current under the applied ac field. This highly localized resistive heating was right at the center of the sample where happened to be the location of the thermometer. While our ac loss measurement was based on the thermometer response and assumed a uniform temperature profile, the ac loss measured for sample D should not be considered as a global behavior of the whole sample.

To confirm this analysis, a new sample (sample E) was fabricated and measured. Instead of at the center, the virtual cross-cut of sample E was at a position near the end of the filaments. The ac loss of sample E, shown also in Fig. 9, was low and comparable to that of sample D*. Both sample D* and E showed almost exactly same ac loss behavior as that of sample B which was fully filamentized from end to end. This would suggest that the heating from the current transfer was highly localized and affected the measurement of sample D. Given that the stabilization of the tested YBCO coated conductors consisted only of silver, the effective thermal conductivity of the characterized conductors was fairly low. With this low thermal conductivity, localized heating only impacts the temperature profile within 1-2 cm, which has been confirmed through 1-D finite difference modeling. So by moving the virtual cross-cut away from the center to the end of the filaments, the drop in measured ac loss in sample E would support that the observed increase in ac loss in sample D was due to this localized heat generation. This also emphasizes that the insertion of the virtual transverse cross-cut can cause a measurable rise in temperature that needs to be studied further to determine its ramifications on conductor performance.

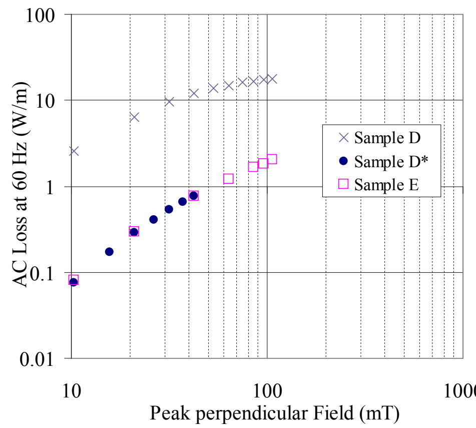

Fig. 9. AC loss measurement results of the three samples that had different configurations. The configurations of sample D and E are as indicated in Fig. 2. Sample D* was made from sample D by removing the silver bridge right above the cross-cut using chemical etching.

IV. CONCLUSIONS

It was demonstrated that a virtual cross-cut in the superconducting layer of an YBCO-based coated conductor could be made by first laser scribing the surface of the IBAD-MgO template and then depositing the HTS film and the subsequent stabilizing silver. Magnetic field distribution study, MOI inspection and magnetization measurements indicated that this cross-cut facilitated the magnetic flux penetration in between the filaments which, in this work, were formed by laser scribing the HTS and the silver layer directly. The improved flux penetration had an effect in further magnetically decoupling the filaments which is a technical issue for long-length tapes when filamentization is used as an approach to reduce ac losses. Preliminary results obtained from short samples that had the geometries simulating long-length tapes showed that the presence of a virtual cross-cut could effectively reduce the hysteresis loss in the filamentized coated conductors. The practical implementation of this approach relies on the tradeoff between the reduction of the hysteresis loss and the induced resistive loss which is due to the introduced resistive bridge right above the virtual cross-cut. Further experiments and analysis are needed to quantify the losses contributed from different mechanisms. The optimization of the cross-cut geometry is also needed to minimize the resistive loss. Future experiments need to be carried on loner length tapes or prototype coils that better reflect the conditions of real applications.

Compared with scribing directly on HTS film and stabilizer layer, making a virtual cut in the coated conductor is much easier in the control of the processing. Therefore, this approach could also be utilized for the filamentization of the coated conductors.

ACKNOWLEDGMENT

The authors are grateful to Professor D. Larbalestier and Dr. A. Polyanskii of Florida State University/National High Magnetic Field Lab (NHMFL) for their help in magneto-optical imaging of the samples. Suggestions from and discussions with Dr. J. R. Thompson and Dr. D. K. Christen of ORNL on SQUID measurements are also greatly appreciated.

REFERENCES

[1] T. Aytug, M. Paranthaman, A. Goyal, and V. Selvamanickam, "ORNL/SuperPower CRADA: Development of MOCVD-based, IBAD-2G Wire," 2010 U.S. DOE-OE Advanced Cables and Conductors Program Peer Review. Available: http://www.htspeerreview.com.

[2] W. J. Carr, Jr., and C.E. Oberly, "Filamentary YBCO conductors for ac applications," *IEEE Trans. Appli. Supercond*. vol. 9, pp. 1475-1478, Jun. 1999.

[3] N. Amemiya, S. Kasai, K. Yoda, Z. Jiang, G. A. Levin, P. N. Barnes, and C. E. Oberly, "AC loss reduction of YBCO coated conductors by multifilamentary structure," *Supercond. Sci. Technol*. vol. 17. pp. 1464-1471, Nov. 2004.

[4] G. A. Levin, P. N. Barnes, and J. W. Kell, "Multifilament YBCO coated conductors with minimized coupling losses," *Appli. Phy. Lett*. vol. 89, pp. 01256, Jul. 2006.

[5] K. Suzuki, J. Matsuda, M. Yoshizumi, T. Izumi, Y. Shiohara, M. Iwakuma, A. Ibi, S. Miyata, and Y. Yamada, "Development of a laser scribing process of coated conductors for the reduction of ac losses," *Supercond. Sci. Technol*. vol. 20, pp. 822-826, Jul. 2007.

[6] M. Marchevsky, E. Zhang, Y. Xie, V. Selvamanickam, and P. G. Ganesan, "AC losses and magnetic coupling in multifilamentary 2G HTS conductors and tape arrays," *IEEE Trans. Appli. Supercond*. vol. 19, pp. 3094-3097, Jun. 2009.

[7] R. C. Duckworth, M. P. Paranthaman, M. S. Bhuiyan, F. A. List, III, and M. J. Gouge, "AC losses in YBCO coated conductor with inkjet filaments," *IEEE Trans. Appli. Supercond*. vol. 17. pp. 3159-3162, Jun. 2007.

[8] C. E. Oberly, L. Long, G. L. Rhoads, and W. J. Carr Jr., "AC loss analysis for superconducting generator armatures wound with subdivided Y-Ba-Cu-O coated tape," *Cryogenics,* vol. 41, no. 2, pp. 117-124, 2001.

[9] O. Tsukamoto, N. Sekine, M. Ciszek, and J. Ogawa, "A method to reduce magnetization losses in assembled conductors made of YBCO coated conductors," *IEEE Trans. Appli. Supercond.* vol. 15, no. 2, pp. 2823-2826, 2005.

[10] D. Abraimov, A. Gurevich, A. Polyanskii, X.Y. Cai, A. Xu, S. Pamidi, D. Larbalestier, and C. L. H. Thieme, "Significant reduction of AC losses in YBCO patterned coated conductors with transposed filaments," *Supercond. Sci. Technol.* vol. 21, pp. 082004, 2008.

[11] S. Ashworth, and F. Grilli, "A strategy for the reduction of ac losses in YBCO coated conductors," *Supercond. Sci. Technol.* vol. 19, pp. 227-232, Jan. 2006.